

# Optical Measurements of Toner Motion in a Development Nip

Howard Mizes,<sup>▲</sup> Jim Beachner and Palghat Ramesh<sup>▲</sup>

Xerox Corporation, Webster, New York

---

In single component development, a monolayer of charged toner is put on a donor roll and presented to a charged image on a photoreceptor. The donor and photoreceptor can either be put in contact or development can occur across a small gap between the photoreceptor and the donor roll. When there is a gap, one can directly observe the toners traversing the gap optically. We have designed a system where we capture the image of the transmitted light through the development gap with a high resolution CCD camera. From these digital images, we can quantitatively extract the toner density, toner size and toner velocity as the particles traverse the nip. Using time delay photography with microsecond resolution we measure the response of the cloud to incoming images. Using an organic film, which can form a permanent latent image, we are able to capture images of fine line development. Quantifying the density and motion of toners in single component development across a gap has allowed us to generate accurate physical models of the development process.

Journal of Imaging Science and Technology 44: 210–218 (2000)

---

## Introduction

### Single Component Development

Development of electrostatically created images requires toner to be charged and then presented to the image. Dual component development systems were created to separate these two steps. In dual component development systems, toner is transported to the development nip on larger, magnetic carrier particles. The carriers provide a means to charge, contain, and transport a large number of toners for development.

A simpler system used in many low end products is single component development (SCD). In SCD, the toner is transported to the development nip on a donor roll.<sup>1,2</sup> The toner must be charged and a number of ways have been devised to do this, including corona charging, contact electrification, induction charge, and control of charge by toner conductivity. The toner adheres to the donor via its electrical image force.

The toner is presented to the latent image either in contact or across a gap.<sup>3,4</sup> Developing across a gap is thought to provide a gentler means to develop toner resulting in higher image quality. The shear forces that are present in contact development do not exist when there is a gap.

Toner can be removed from the donor roll and transported to the photoreceptor by applying a combination of AC and DC electric fields. Toner will move across the nip and remain on the photoreceptor in the image areas. Quite large fields are required to move the toner and development in the background region can occur.

Alternatively, a powder cloud can be generated in the nip region. The toner cloud is created by using a combination of mechanical and/or electrostatic means that suspend toner in the nip region. Toner is pulled from the cloud reservoir to develop a latent electrostatic image. The shape and density of the toner cloud can be controlled giving more opportunities to improve image quality.

### Cloud Visualization

Single component development across a gap provides an opportunity to observe the development of toner in a way not possible with other development techniques. The nip region can be illuminated with a light source and imaged with a high magnification microscope. Using digital image capture techniques, one can observe and quantify the dynamics of the toner in the nip region. In Fig. 1, we show the experimental setup that we call cloud visualization used to monitor the development of toner.

The cylindrical donor roll is shown in cross section in the figure. It is loaded with charged toner and continuously rotated to bring the toner to the development nip. At the 12 o'clock position is a cloud generation mechanism, where toner is removed from the donor and suspended in the nip. In most of our experiments, a metallic cylinder is used as a surrogate for the photoreceptor. Development occurs if the receiver is biased to attract toner and development is turned off if the roll is biased to repel toner. The amount of developed mass can be controlled by the magnitude of the voltage difference between the receiver and the donor.

A camera is attached to high magnification optics and focussed onto the nip. Light is transmitted through the nip and imaged with the camera. A toner blocks the light and appears as a circular shadow in the nip region. If the toner does not move appreciably while the camera shutter is open, it will appear fixed as it does in the image as shown in Fig. 1.

---

Original manuscript received October 25, 1999

▲ IS&T Member

©2000, IS&T—The Society for Imaging Science and Technology

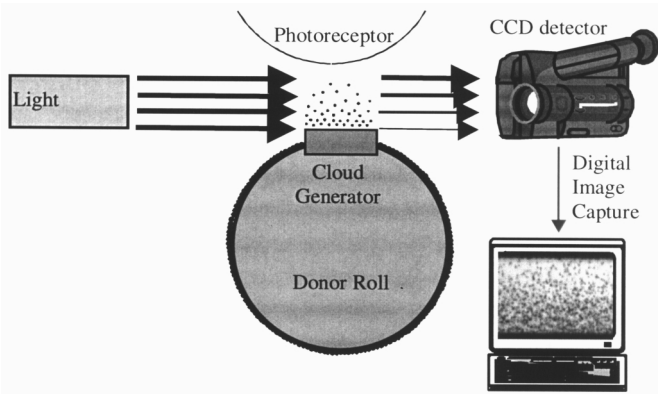


**Figure 1.** Cloud visualization apparatus. The light source is a high intensity incandescent source placed far from the nip with a diffuser plate in order to provide uniform illumination. A high magnification lens system with a working distance of 3 inches is attached to one of two cameras: a camera collected interlaced video at a standard speed of 30 frames/sec, or we used a still camera with an electronic shutter adjustable between 1  $\mu$ sec and 1 msec.

The width of the powder cloud is the distance along the donor roll rotation direction the cloud is active. If the width of the powder cloud exceeds the depth of focus, then toner particles may appear blurred. This decreases the resolution of cloud visualization. For the images presented in this article, the width of the powder cloud is less than or on the order of the depth of focus.

Other researchers have published results on the motion of toners observed optically. Yamamoto and co-workers<sup>5</sup> looked at the motion of individual toners between parallel plates when an electric field was applied to cause the toners to jump from one plate to the other. They collected images at a rate of 4000 per second with a high speed camera and could determine the trajectories and speeds of selected toners. Takehashi and co-workers<sup>6</sup> also performed visualization experiments in the early 1980's.

The new work that we are presented here is our observation of toner motion in a real development system. We also perform a level of quantitative image analysis that allows a characterization of development in such a way to provide inputs to physical models, and to determine fundamental critical parameters of powder cloud development.

We begin with a discussion on how both individual particles and the average cloud density can be observed by varying the camera shutter speed. From the images of individual particles, the particle sizes in the nip can be obtained. At slightly longer shutter speeds toner streaks are observed and from these streaks the toner velocities can be determined. When the shutter remains open for a long time the average cloud density is obtained, and from the image the toner volume fraction is calculated. We give an example of how this information can be used to calculate the launch velocities of toner into the nip region. Following this discussion, we give two experimental examples of determining dynamics of the development system: the response of the cloud to a development field, and the response of the cloud to a latent image of a line.

## Results and Discussion

### Shutter Speed Effect

The nature of the cloud visualization image will change based on how long the shutter of the camera is

open. If the shutter speed is short compared to the velocity of the toner, the toner does not move significantly while the shutter is open. The individual toners block the transmitted light and appear black. If the shutter is left open longer, the toners can move during the time the shutter is open. The toners appear as streaks, where the beginning of the streak is the position of the toner when the shutter is opened, and the end of the streak is the position of the toner when the shutter is closed. The longer the shutter is left open, the longer the streaks become. As the streaks become longer, they also become lighter, because the toner spends less time obstructing the light path to each pixel.

As the time the shutter remains open continues to increase, the trails become longer and longer and begin to overlap to where it becomes impossible to resolve individual toners. At even longer times, so many toner enter and leave the field of view that the response of each camera pixel corresponds to the average amount of time that the pixel is obstructed by a toner. The gray level of the camera pixel corresponds to the density of toner at that particular region in space.

We can estimate the time scale of these transitions by determining the velocity of individual toners. The top speed of a toner in the nip is given by Stokes law.<sup>7</sup> Stokes law states that the repelling force acting on a toner moving at velocity  $v$  is

$$F_{stokes} = 3\pi\eta dv \quad (1)$$

where  $\eta$  is the viscosity of air (1.8 Pa-sec),  $d$  is a toner diameter (typical value is 10  $\mu$ m) and  $v$  is the toner velocity. The force driving the toner to the other electrode is  $F_e = qE$ , where  $q$  is a toner charge (typical value is  $10^{-14}$  Coulombs) and  $E$  is the electrical field in the nip region (typical value is  $10^6$  Volts/meter). The toner terminal velocity occurs when  $F_e = F_{stokes}$ . Using the typical values from above, we find the terminal velocity of a typical toner to be 6 m/sec. In applying Stokes law, we assume that the roll motion does not cause air to flow in the nip region.

As a toner develops, it will accelerate from its velocity in the cloud as it moves towards the photoreceptor and may not reach its terminal velocity. However, for a shutter speed of 1  $\mu$ sec, the toner will at the fastest move about half its radius and we should be fairly certain that we should be able to freeze the toner motion. In Fig. 2 we show three images of the nip region with shutter speeds of 1  $\mu$ sec, 5  $\mu$ sec, and 1 msec, respectively. In these images, the donor roll is on the bottom of the image and the receiver roll is on the top of the image. The receiver roll was modified so toner is attracted only to a portion of the roll in the center of the image (the technique will be described in more detail in the section on imaging lines). For the 1  $\mu$ sec shutter speed, the toners are seen not to move while the shutter is open and appear as black dots. If the shutter speed is increased to 5  $\mu$ sec, the toners move and appear as streaks. The motion appears to be most rapid at the edge of the developing line. For a shutter speed of 1 msec, the toner moves so much during the image so that only a cloud appears, with the gray level corresponding to the amount of time that toner is located at a given position in the nip.

### Particle Size Measurements in the Nip

In order to understand the dynamics of powder cloud development, it is important to know the toner sizes in the nip. The size distribution of toner in the nip doesn't necessarily have to be the same as the toner size dis-

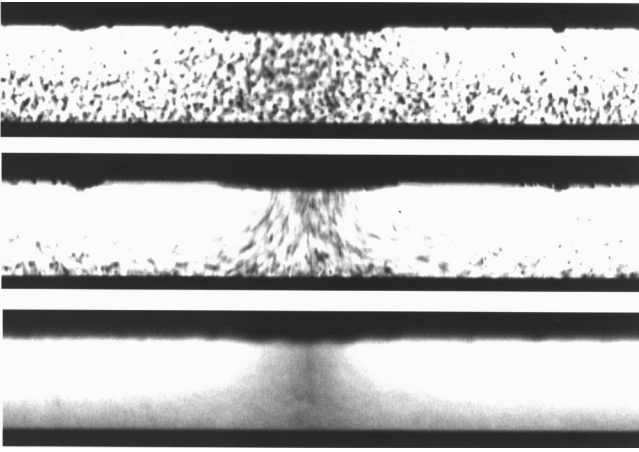


**Figure 2.** Images of the toner cloud taken at different shutter speeds. The donor roll is on the bottom and the receiver is on the top. The center of receiver is charged to attract toner, and the sides are charged to repel toner: (a) Shutter speed of 1  $\mu$ sec. The toners are frozen in place. (b) Shutter speed of 5  $\mu$ sec. Streaks indicate developing toner is moving up to 10 m/sec. (c) Shutter speed of 1 msec. Long exposure gives stable cloud of average positions.

tribution on the donor or in the sump. The efficiency of loading toner on the donor roll and of removing toner from the donor into the cloud may be toner size dependent.

The diameter of the toner in an image such as Fig. 2a cannot be directly measured. The size of the toner is close to the pixel dimensions of the magnified image. For our high-speed camera, which has an asymmetric pixel size, the pixel dimension is  $3.0 \times 7.0 \mu\text{m}$ . Also, for a toner in the image plane, its appearance will be modified by the diffraction of light around the edge of the toner. In addition, because the cloud has a finite width, not all the toner will be in the image plane. The toner will be out of focus, which will give it the appearance of an Airy disk.

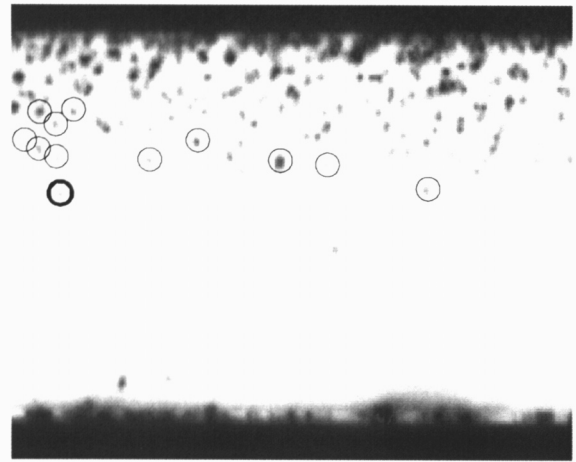
However, the gray level response of each pixel integrated over the area covered by the toner will be independent of diffraction and the degree of focus. Let the camera pixel have a size  $p_x$  by  $p_y$ . The response of each camera pixel  $i, j$  is converted to a value  $a_{ij}$ , where  $a_{ij}$  represents the attenuation of the light by the toner. Because of the blurring, no pixel is completely obstructed. The total area is found by summing the fraction of the toner obstructing each pixel and is

$$a_t = p_x p_y \sum_{i,j} a_{i,j} \quad (2)$$

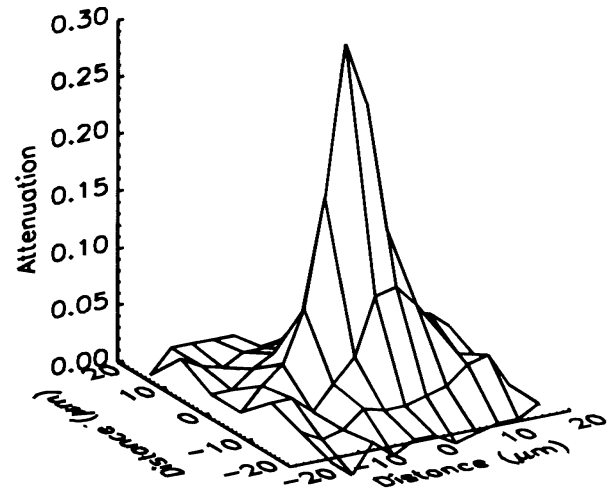
From the area, the toner diameter is

$$d_t = 2 \sqrt{\frac{a}{\pi_t}} \quad (3)$$

We tested this algorithm on a 1  $\mu$ sec shutter image of the cloud. We identify the location of isolated toners manually and extract them from the figure. To calculate the attenuation, we need to know what the camera pixel response is for no toner present. Also the presence of neighboring toners can attenuate light near the test toner and the sum of attenuations may be overestimated. In order to minimize the errors introduced



(a)



(b)

**Figure 3.** (a) Image of a cloud taken with a 1  $\mu$ sec exposure speed. Isolated particles for which the diameter was measured are circled. (b) Surface plot of the attenuation corresponding to the particle with the bold circle. The pixel dimensions are  $7.0 \mu\text{m} \times 3.0 \mu\text{m}$ . The light is spread over many pixels, but the integrated intensity corresponds to particles of diameter approximately  $7.5 \mu\text{m}$ .

by these effects, we fit a product of two Gaussian functions in the horizontal and vertical dimension to the toner image. The parameters of the Gaussian are the background gray level  $b$ , the amplitude  $\Delta p$ , the horizontal and vertical position of the center of the toner,  $i_0$  and  $j_0$ , and the widths in the horizontal and vertical direction  $\Delta i$  and  $\Delta j$ . The function is

$$a_{ij} = b - \Delta p e^{-(i-i_0)^2 / \Delta i^2} e^{-(j-j_0)^2 / \Delta j^2}. \quad (4)$$

The Gaussian can be numerically integrated to give the total attenuation. From the total attenuation, the area of the toner is

$$a_{\text{toner}} = \frac{\Delta p \Delta i \Delta j \pi p_x p_y}{b}. \quad (5)$$

Figure 3a shows a section of a cloud visualization image taken with a 1  $\mu$ sec shutter speed. From this im-

age, we identified 12 toners non-overlapping with other toners and used the above equations to determine their diameters. Arrows identify the toner in the image. Figure 3b shows the gray level of the particle, indicating that it is well approximated by a Gaussian. We found the average diameter to be  $7.45 \mu\text{m}$  with a standard deviation of  $2.59 \mu\text{m}$ .

### Detecting Toner Density Using the Transmitted Light

We now turn to quantifying cloud visualization images taken using long shutter speeds, when the individual toners are not resolved. For clouds with a low volume fraction of toner, the light transmitted is proportional to the number of toners in the cloud, because toners do not overlap and shadow each other. Consider, a cross-section area  $a_{cs}$  of the cloud that contains  $N$  toner particles in a nip width  $w$ . Assuming spherical particles, the light absorbed by each particle is equal to  $\pi r^2$ , where  $r$  is the particle radius. Thus the attenuation of light through the cloud as low volume fractions, approximately  $a = N\pi r^2/a_{cs}$ . Now the volume fraction is  $\phi = NV_p/(a_{cs}w)$ , where  $V_p$  is the volume of a toner particle, i.e.,  $V_p = 4\pi r^3/3$ . Thus attenuation is  $a = 3\phi w/4r$ , or  $da/d\phi = 3w/4r$ .

For higher volume fractions, the transmitted light obeys Beer's law<sup>8</sup> and the attenuation may be written as  $a = 1 - \exp(-\alpha\phi)$ , where  $\alpha$  is a constant. In the limit as  $\phi \rightarrow 0$ ,  $da/d\phi = \alpha$ , thus  $\alpha$  is set to  $3w/4r$  to match the low density result. The volume fraction is, therefore,  $\phi = -4r \log(1 - a)/3w$ .

Cloud width,  $w$ , and volume fraction of toner,  $\phi$ , can both vary as a function of the height,  $z$ , above the donor, and location,  $x$ , along the donor. The image wise attenuation,  $a(x, z)$ , is measured by comparing the transmitted light intensity from the camera signal with and without toner in the nip. The number density projected onto the  $x$ - $z$  plane,  $N(x, z)$ , can then be calculated from  $a(x, z)$ .

We can use this formalism to characterize the toner density as a function of the development voltage. The development voltage, which is the voltage difference between the donor and the receiver, controls the amount of toner that develops to the receiver. At higher development voltages, more toner must deposit on the photo-receptor to neutralize the image. In regions where there is no image, the voltage difference between the receiver and the donor is set to repel toner. The larger the repelling field, the closer the cloud will move towards the donor. In real development systems, this sort of control of the toner cloud will affect background development, the response time of the cloud to an incoming image, and line shrinkage. We use cloud visualization to monitor the cloud height experimentally.

We can present the cloud in a more quantitative way by taking the cross section of the image in the vertical direction, that is, between the donor and receiver. Each point in the image is averaged in the horizontal direction. (Using the known camera magnification, the pixel spacing is converted to distance.) A typical cloud profile is plotted in Fig. 4.

The profile contains artifacts due to diffraction and reflection at the donor and receiver surface. This causes oscillations in the light intensity near the edge of the receiver. We remove these oscillations by fitting the signal to the function

$$s(z) = A(1 - e^{-(z-b)/c}), \quad (6)$$

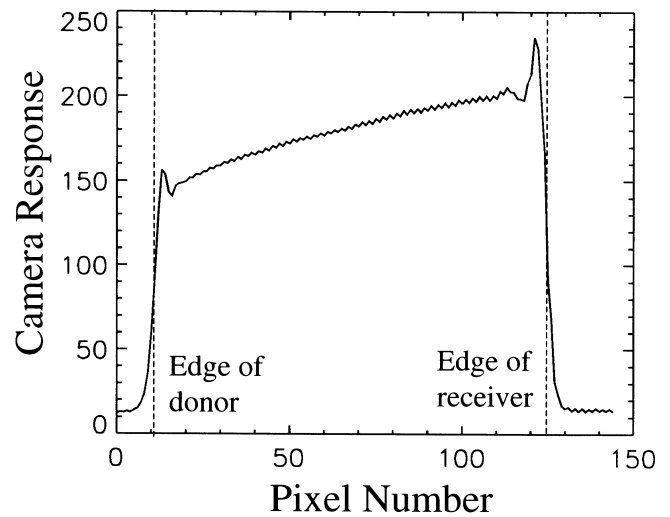


**Figure 4.** Camera response versus distance across nip averaged parallel to the donor surface. Large numbers correspond to higher transmission.

where  $A$ ,  $b$ , and  $c$  are adjustable constants to fit the data,  $z$  is the distance from the donor roll, and  $s(z)$  is the signal from the camera. For large  $z$ , the signal approaches  $A$ . Large  $z$  is far from the donor roll where there is little toner. Therefore,  $A$  may be interpreted as the intensity of the unattenuated incident light, integrated over the imaging time.

Note that the attenuation thus calculated may be sensitive to the inaccuracies in the exponential fit. A better technique would be to use data directly from a no-cloud image to get  $A$ . However, instabilities in either the light source intensity, the camera shutter speed, or some other factor has caused the maximum exposure to vary, and the technique described above gives a more accurate estimate of the unattenuated light intensity.

Using the above equations and an estimate of the width of the toner cloud, we convert the measured images of the cloud to volume fraction of toner. The volume fraction is plotted as a function of height for a series of cleaning voltages in Fig. 5. We see that the higher voltages significantly compress the cloud closer to the donor roll.

### Extraction of Toner Velocities

Measurement of the velocities of individual toner particles as they traverse the nip aids in understanding the development process. The balance between electrostatic forces and the Stokes drag force associated with air resistance determines the terminal velocity of toner particles. Understanding the interplay between these forces gives information about how development changes for different size toner particles in different electric fields. For example, smaller toners are expected to increase image quality, but they may move across the nip too slowly to adequately develop fine lines and fill in line edges.

Modeling these effects requires an expression for velocity of toner moving across the nip. However, this is not easily estimated without an experiment. Toner encounters drag due to the air, but the form of the drag depends on toner density, shape, and air flow in the nip, and can be of many forms. Each of these forms may give estimates of the velocity that differ an order of magnitude.

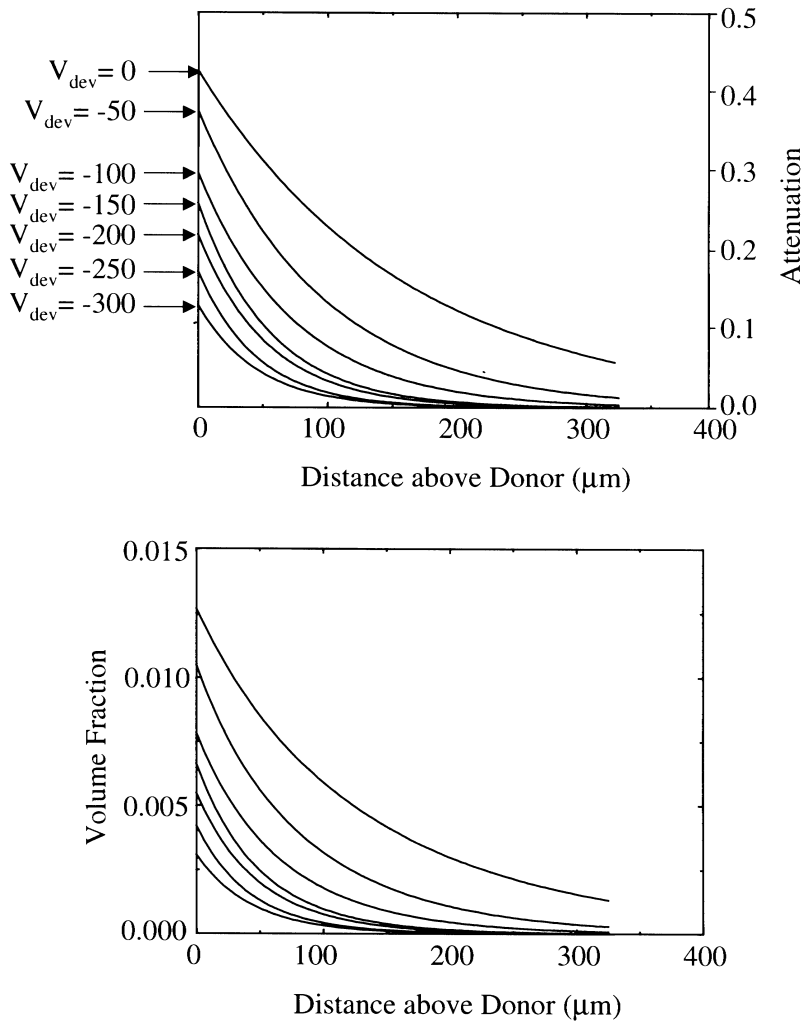


**Figure 5.** (a) Light attenuation versus position in the nip for a series of different cleaning fields. (b) Attenuation data converted to toner volume fraction using an estimate of the cloud width.

Using the cloud visualization apparatus, we measured the velocity of toner moving across the nip in different development fields. We chose a shutter speed of 100 μsec, which gave streaks of a measurable length.

As the toner moves, it will appear as a streak in the image. From the length of the streak and the shutter speed, we can calculate the velocity. The amount of toner in the cloud was controlled and lowered to give little toner overlap where individual particles were easily identified. Four measurements were made at development voltages of 50, 150, 250, and 350 V. The images are shown in Fig. 6a.

Twenty particle tracks were measured in each image. The clearest particles were chosen. Particles whose path ended on the receiver were excluded to guarantee they were not at rest while the shutter was open. Paths that ended near the receiver were preferred because this is where the field is most uniform. From the length of the paths we determined the velocity. The median velocity of the 20 measured paths from each image is plotted as a function of development voltage in Fig. 6b.

### Extraction of Toner Launch Velocities

Another use of the visualization apparatus is to extract toner launch velocities, i.e. the velocities with which toners are launched into the gap by the cloud generator (see Fig. 1). This velocity is dependent on the cloud generation mechanism and may be a useful metric to evalu-

ate the cloud generator. In simplistic terms, the cloud generator provides initial kinetic energy to the toners that are then further accelerated in a development field or decelerated in a cleaning field. We discuss here an indirect way to infer toner launch velocities from cloud images.

In the absence of hydrodynamic drag, the total energy  $TE$  (kinetic + potential) is conserved for each particle i.e.,

$$TE = \frac{1}{2}mv(z)^2 + qV(z) = \frac{1}{2}mv_0^2 \quad (7)$$

or

$$v(z) = \sqrt{v_0^2 - 2V(z)(q/m)} \quad (8)$$

Here  $v$  is the toner velocity at height  $z$  above the cloud generator, and  $V$  is the electrostatic potential referenced with respect to the cloud generator.  $q$  and  $m$  are the toner charge and mass, respectively.  $v_0$  is the initial launch velocity.  $V$  depends on the applied bias ( $V_{dev}$ ) and space charge in the cloud. Thus

$$v_{0,max} = \sqrt{2V_{dev}(q/m)}$$

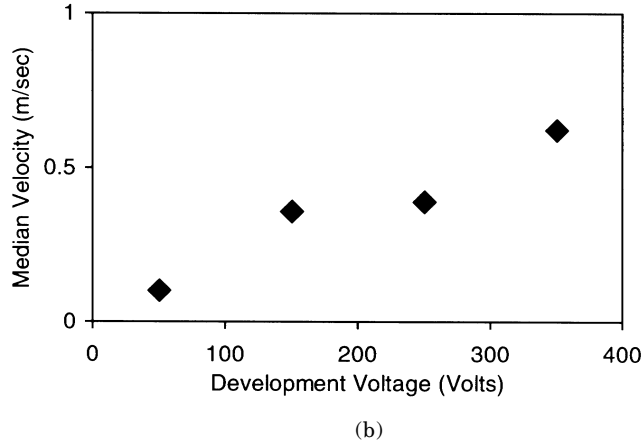
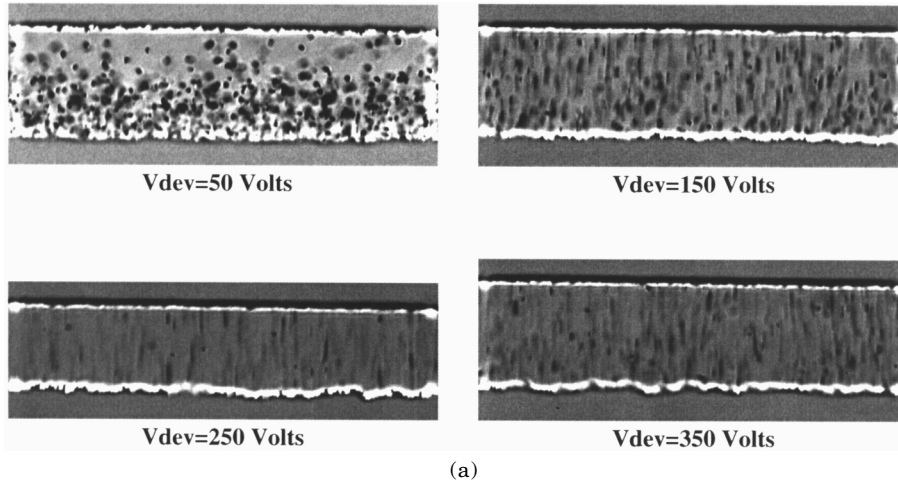


**Figure 6.** (a) Cloud visualization images with an exposure of 100 msec for different development voltages. At higher development voltages the toners move faster and appear as longer streaks. (b) Median velocity inferred from measuring the streak length of 20 particles in each image.

is the minimum initial launch velocity needed to reach the receiver. Toners with launch velocity greater than  $v_{0,max}$  can develop on the receiver and those with launch velocity less than  $v_{0,max}$  will turn around before reaching the receiver. Initial launch velocity of the toner that turns around at  $z$  is

$$v_0(z) = \sqrt{2V(z)(q/m)} .$$

Let  $E$  be the kinetic energy of the toner. Define  $E_{0,max} = 2V_{dev}(q/m)$  and  $E_0(z) = 2V(z)(q/m)$ . Consider a distribution function  $f_0(E)$ , where  $f_0(E)dE$  is the fraction of all the toners launched with initial kinetic energies between  $E$  and  $E + dE$ .

Let  $\phi(z)$  be the toner volume fraction in the gap that may be calculated from the cloud images as mentioned before. One can easily solve for the electrostatic potential distribution in the gap,  $V(z)$ , by solving the Poisson's equation:

$$\frac{d^2V}{dz^2} = -\frac{\rho}{\epsilon} = -\frac{\phi(z)(q/m)\rho_{mt}}{\epsilon} , \quad (9)$$

where  $\rho_{mt}$  is the toner mass density, and  $\epsilon$  is the permittivity.

The toner density at height  $z$  is a sum of the toners that just make it to height  $z$  and the toners that pass

through  $z$  on their way up and down. Also, the relative contribution of a toner traveling through  $z$  to the volume fraction  $\phi(z)$  is inversely proportional to its velocity at  $z$ . This can be stated mathematically as follows:

$$\phi(z) = I_0 V_t \sqrt{\frac{m}{2}} \left\{ 2 \int_{E_0(z)}^{E_{0,max}} \frac{f_0(E)}{\sqrt{E - E_0(z)}} dE + \int_{E_{0,max}}^{\infty} \frac{f_0(E)}{\sqrt{E - E_0(z)}} dE \right\} \quad (10)$$

where  $V_t$  is the volume of a toner particle, and  $I_0$  is the injection rate at  $z = 0$ , i.e., the number of toners injected per unit area per unit time. The first integral on the left hand side is due to toners not reaching the receiver (and hence the factor 2 to account for contributions from toners moving up as well as down). The second integral is the contribution from toners reaching the receiver. In general, we do not have sufficient information to extract  $f_0(E)$  from  $\phi(z)$  distribution. However, in a strict cleaning regime, the second integral should be 0 (no toners reach the receiver), and in this case  $f_0$  can be extracted from  $\phi$ . The analysis can be easily extended to include air drag. Figure 7a shows a plot of computed  $f_0(E)$  for

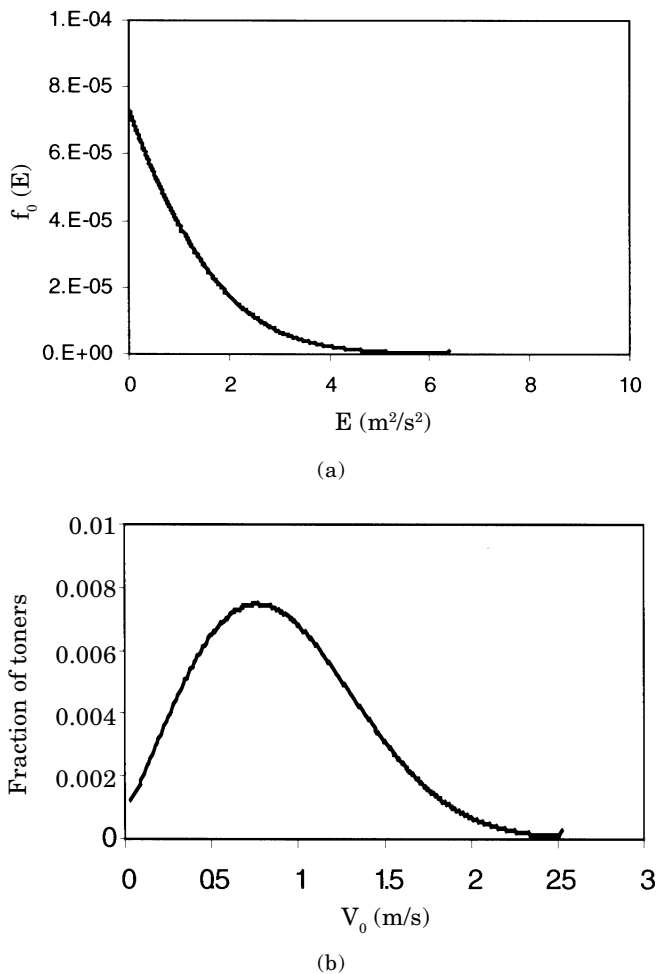


**Figure 7.** Toner launch velocity distributions computed from cloud visualization image for  $V_{dev} = -200V$ . (a) Launch kinetic energy distribution  $f_0(E)$ . (b) Launch velocity distribution of particles.

$V_{dev} = -200V$ . The corresponding launch velocity distribution is shown in Fig. 7b. The computed injection rate of toners at the generation electrode is  $I_0 = 3.2 \times 10^{12}$  toners/m<sup>2</sup>/s. These parameters serve as inputs to developability models such as the one discussed in Gartstein and Ramesh.<sup>11</sup>

### Cloud Response Time

The motion of a toner cloud in response to an electrostatic image has direct consequences for image quality. For example, imagine a single pixel latent image running parallel to the donor roll coming into the nip. If the cloud responds too slowly, the line will pass through the nip before the cloud can rise, and the line will be underdeveloped. Another example is an edge of a solid parallel to the donor roll. Part of the edge may pass through the nip before the cloud rises to start developing and the leading edge of the image will not be fully developed.

A high speed camera that could take a full image of the development nip with 10  $\mu$ sec resolution between images would have the capability of taking a video of the cloud evolving as the receiver was switch from a cleaning field to a development field. We did not have the capability to perform this experiment. However, the cloud response time measurement is repeatable, so we

performed the experiment as follows: The receiver is biased to repel toner. At time zero, the receiver voltage is switched to a developing field. At an adjustable time  $\Delta t$  after the receiver roll bias is switched, an image of the cloud is taken at the shortest possible shutter speed. The experiment is repeated for a series of  $\Delta t$ 's, from  $\Delta t = 0$  to a large  $\Delta t$  at which the development is occurring to completion. The cloud on average is expected to respond the same way. A subset of these images for a particular value of voltage differences across the nip is shown in Fig. 8a.

From these images, we can extract the midpoint of the cloud. The midpoint of the cloud is defined as the point where 50% of the toner in the visible nip region lies below this point and 50% of the toner lies above this point. The cloud midpoint will rise as the cloud rises to develop an image.

To test the capability of the cloud response time experiment, we measured the cloud dynamics for a 500 V change in the receiver bias. The 50% midpoint versus  $\Delta t$  is plotted in Fig. 8b. The diamonds are the metrics from the individual images, and the solid line is a fit of the function  $f = h_0 + \Delta h(1 - \exp(-\Delta t/t_0))$  to the data, where  $h_0$  is a measure of the initial height of the cloud, and  $t_0$  is a measure of the temporal response of the cloud to the development field. We have used this technique to study the sensitivity of the cloud response time to electric field strength and toner charge to mass ratio.

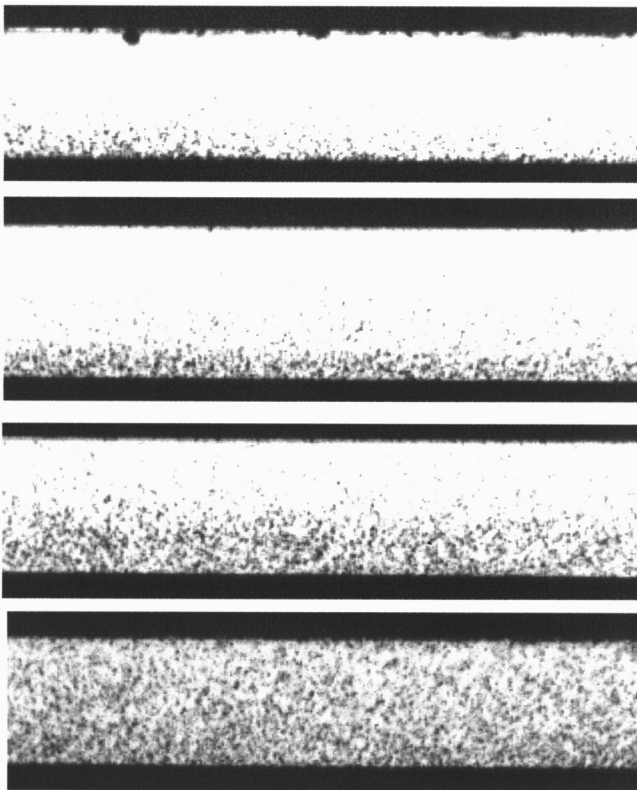
### Development of Fine Lines

High quality printing requires the accurate development of fine lines. Line shrinkage or line growth can occur if the development parameters are not optimized. Half-tone dot gain is also associated with controlling line development. The cloud visualization technique can be used to examine the relationship between the cloud and the line widths developed.

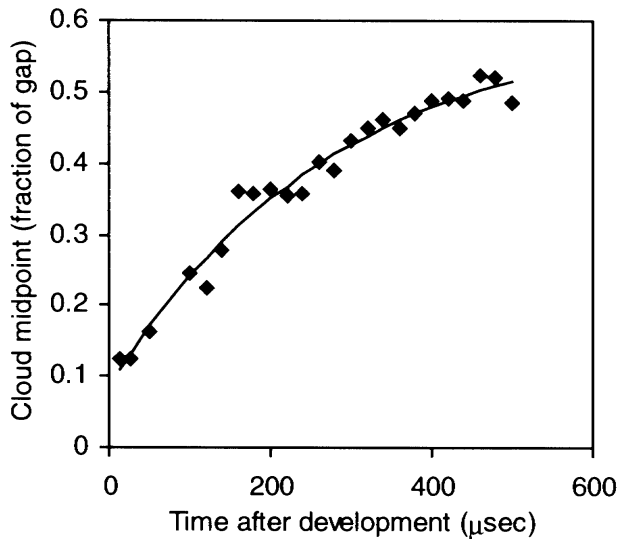
In a xerographic printer, lines are created in latent images by exposing a photoreceptor with light from a laser ROS or an LED bar. We chose an alternative method of creating lines to develop which made the experiment simpler. We attached a special material called Verde Film to the receiver, which has a permanent latent image.<sup>9</sup> The permanent latent image is created prior to the experiment by exposing the film to ultraviolet light through a mask. Selenium ions that are initially on the film surface of the insulating film migrate through the film rendering the film conduction. Areas of the Verde Film that have been exposed to ultraviolet light are then unable to hold a charge. An electrostatic latent image can therefore, be created by charging a biased film. We used an 8  $\mu$ m thick film upon which a 100  $\mu$ m wide line was written and attached it to the receiver as shown in Fig. 9.

As the line passes through the develop nip, toner is pulled from the cloud and develops to the line. An image of this process is shown in Fig. 10a. The bump on the receiver roll extending into the nip is an image of the developed line looking edge on. The image of the gap to either side of the developing line is lighter at the top, indicating the cloud resides near the toner supply surface in regions where no image is being developed.

The height of the line as a function of position along the receiver can be determined from the digital image. A series of vertical cross sections of the image is taken from the left side of the line to the right side of the line. The camera pixel response goes from a value near 255 corresponding to a high transmission of light to a value



(a)



(b)

**Figure 8.** (a) A series of cloud visualization images taken with a 1 μsec shutter speed taken at a delay of 50 μsec, 140 μsec, 200 μsec, and 500 μsec after the receiver roll was switched from a cleaning field to a development field. (b) Median cloud height plotted as a function of time after a development field was turned on.

near 0 where the receiver roll blocks the incoming light. We pick a threshold midway between the light and dark values and determine the pixel at which the threshold is crossed. We linearly interpolate between pixels to increase the resolution of the measurement.

The line profile is shown in Fig. 10b. The full width of the half-maximum can be taken as a measure of the

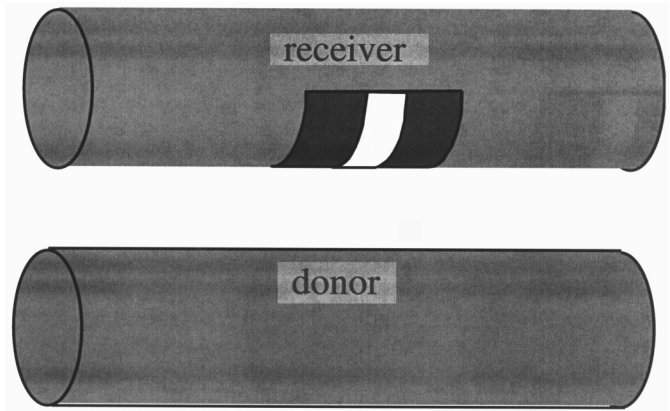
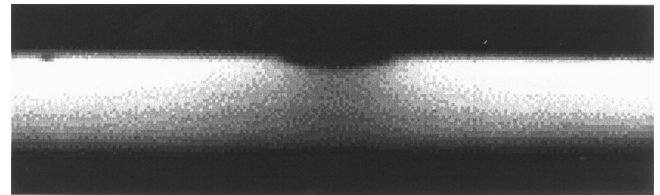
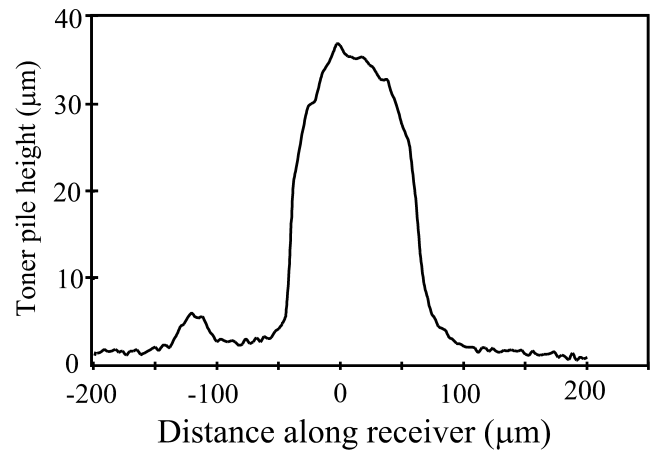


**Figure 9.** Schematic of line development imaging with cloud visualization.



(a)



(b)

**Figure 10.** Cloud visualization image of line developing. The line edge and the developing toner are indicated in the figure.

line width. For the image in Fig. 10b, the line width is 101.5 μm.

A dark region in the image can be observed extending from the cloud to the developed line. The width of this darker region increases closer to the powder cloud supply. This dark region is the toner being pulled from the cloud to develop to the line. It is wider near the donor because toner is being pulled from regions of the cloud greater than the line width.

Figure 11 shows a series of images of a developing line taken at different gaps between the donor and the receiver. As the gap increases, the plume of toner pulled from the cloud continues to shrink in width resulting in a narrower line. Halftone dots would be expected to show the same sensitivity. Therefore development is highly gap sensitive and the gap must be accurately maintained in order to have consistent lines and uniform gray areas.

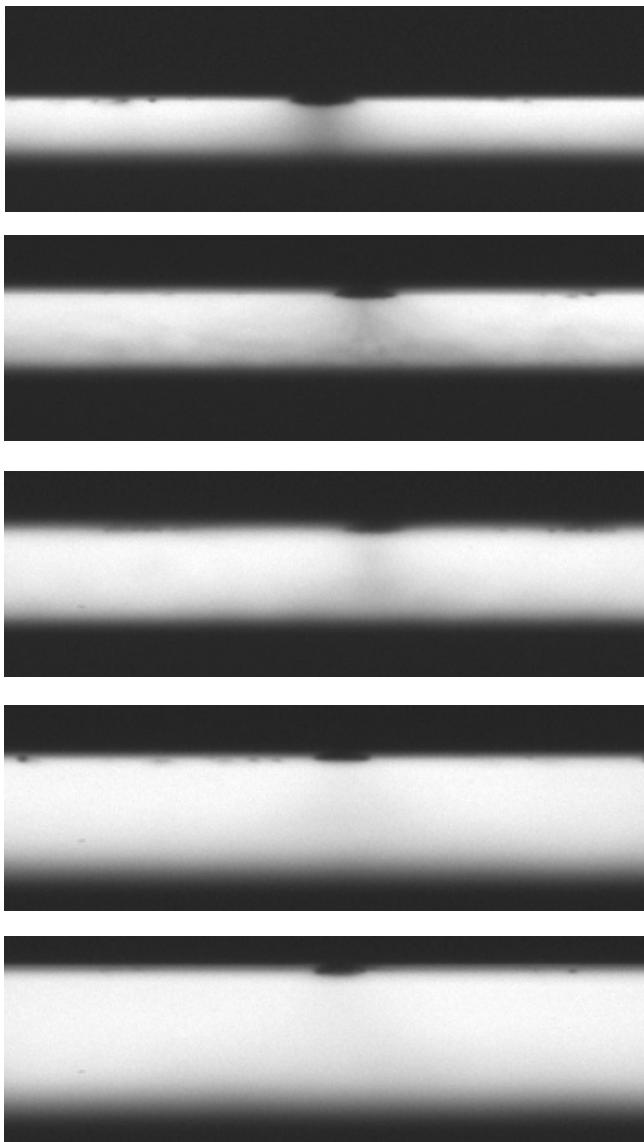


**Figure 11.** Cloud visualization image of line development at different gaps.

## Conclusions

Improving image quality for a development process consists of changing parameters of the development system and observing any beneficial change on the image quality. Models of the development process have assisted in identifying and understanding what controls image quality.<sup>10,11</sup> These models typically used physically based expressions for the transport of particles in the nip and match the parameters to measurements of solid area

development. The solid area development curves allow parameters in the model to be adjusted, but there are more adjustable parameters than experimental parameters to fit.

Cloud visualization allows for a more accurate link between system image quality performance and physical mechanisms. Visualizing the toner motion in the nip cannot only be used to monitor image quality, but also to gain a better perspective of how toner motion can be controlled. In addition, being able to quantify toner densities, and monitor individual toner velocities and the dynamics of the cloud has allowed the development of accurate single particle models of powder cloud development. The model must not only be able to predict solid area development, but also the shape and dynamics of toner in the cloud. This constrains the freedom of choosing arbitrary parameters in the model. Based in part from cloud visualization, highly accurate first principle based models have been developed.<sup>10,11</sup>  $\triangle$

**Acknowledgments.** We would like to thank our Xerox colleagues who have suggested ideas that grew into some of the experiments presented here. Bill Wayman, Ray Stover, and Jeff Folkins did some early experiments demonstrating the usefulness of the technique. John Andrews had numerous suggestions on the optical aspects of the experiments. John Shaw and Yuri Gartstein were key people in developing the modeling tools upon which the calculations presented in this article are based.

## References

1. L.B. Schein, *Electrophotography and Development Physics*, 2<sup>nd</sup> ed., Springer-Verlag, Berlin, 1992.
2. J. Bares, Single-Component Development: A Review, *J. Imaging Sci. Technol.* **38**, 401 (1994).
3. M. Hosoya, S. Tomura and T. Vehara, Xerographic Development Using Single-Component Non-magnetic Toner, *IEEE-IAS 1985 Annual Conf. Record*: 1485-1490 (1985); see also *IEEE Trans. On IAS* **24** (2), 238-243 (1988).
4. Hidekiyo Tachibara, Nobuo Hyakutake and Kazuo Terao, Control of Toner Reproduction Characteristics by Time Constant of Development Roller in Mono-Component Development, *IEEE-IAS 1989 Annual Conf. Record*: 2260-2265 (1989). See also *IEEE-IAS Trans.* **27** (3), 501-506 (1991).
5. Y. Yamamoto, Observation of the Movement of Toner Particles Between Parallel Electrodes, *IS&T's NIP13, International Conference on Digital Printing Technologies*, IS&T, Springfield, VA, 1997.
6. T. Takahashi, H. Hosono, J. Kanbe and T. Toyona, *Photo. Sci. and Eng.* **26**, 254 (1982).
7. G. K. Batchelor, *An introduction to fluid dynamics*, Cambridge University Press, Cambridge, UK, 1967, p. 233.
8. U. Riebel and U. Krauter, Extinction of radiations in sterically interacting systems of monodisperse spheres. Part 1: Theory, *Part. Part. Syst. Charact.* **11**, 212 (1994).
9. Seybold Report on Publishing Systems, Vol. 23, No. 9 (1996).
10. J. Shaw and T. Retzlaff, Particle Simulation of Xerographic Development, *IS&T's NIP12, International Conference on Digital Printing Technologies*, IS&T, Springfield, VA, p. 199; J. G. Shaw and T. Retzlaff, Particle Simulation of Xerographic Line Images, *Proc. IS&T's NIP15: International Conference on Digital Printing Technologies*, IS&T, Springfield, VA, 1999, p. 467.
11. Yu. N. Gartstein and P. S. Ramesh, Hysteresis and self-sustained oscillations in space charge limited currents, *J. App. Phys.* **83**, 2958-2964 (1998).